ELSEVIER

Contents lists available at ScienceDirect

Earth and Planetary Science Letters

journal homepage: www.elsevier.com/locate/epsl





The spatio-temporal evolution of ¹⁸²W and ¹⁴²Nd in the Deccan-La Réunion plume

Josua J. Pakulla ^{a,*} ⁶, Jonas Tusch ^a, Eric Hasenstab-Dübeler ^a, Arathy Ravindran ^a ⁶, Mike W. Jansen ^a ⁶, Felipe P. Leitzke ^{a,c} ⁶, Purva Gadpallu ^b, Raymond A. Duraiswami ^b ⁶, Carsten Münker ^a ⁶

- ^a Universität zu Köln, Institut für Geologie und Mineralogie, 50674 Köln, Germany
- ^b Savitribai Phule Pune University, Department of Geology, 411007 Pune, India
- ^c Universidade Federal de Pelotas, Depto. de Engenharia Geológica, Centro de Engenharias, 96010-540 Pelotas, Brazil

ARTICLE INFO

Keywords: 182W.142Nd isotopes Deccan-La Réunion plume OIB DVP Recycled material LLSVP

ABSTRACT

Variations of the short-lived decay products ¹⁸²W and ¹⁴²Nd that formed approximately during the first 60 and 500 million years after solar system formation are pivotal in our understanding of Hadean processes and homogenization of Earth's mantle. For example, a coupling of ¹⁴²Nd and ¹⁸²W anomalies for the Deccan-La Réunion plume has been previously suggested to mirror a combined involvement of core-mantle interaction and Hadean silicate material, possibly stored in Large Low Shear Wave Velocity Provinces (LLSVPs). However, the limited availability of such short-lived isotope data for basalts from the Deccan Volcanic Province (DVP) made it difficult to assess this model closely. In this study, we provide new combined $\mu^{142}Nd$ and $\mu^{182}W$ data for ten selected samples of the DVP and one TTG from the Dharwar Craton basement, now covering different mantle endmembers of the DVP. Additionally, we provide new $\mu^{142}Nd$ data for six volcanic rocks from La Réunion that were previously analyzed for 182 W. We do not find evidence for a correlation between μ^{142} Nd and μ^{182} W in contrast to previous suggestions. Our data show that the involvement of mantle lithosphere and crustal components influences the μ^{182} W compositions of the DVP samples. Values of μ^{182} W (-4.2 \pm 3.0) of such contaminated DVP samples overlap with the compositional field of volcanic rocks from La Réunion (-4.9 \pm 1.5). The asthenospheric endmember of the DVP displays resolvable larger $\mu^{182}W$ deficits as low as -12.0 \pm 2.3. Additionally, the asthenospheric DVP endmember also displays more unradiogenic $^{206}\text{Pb}/^{204}\text{Pb}$ ratios and low $\Delta^{207}\text{Pb}/^{206}\text{Pb}$ compared to La Réunion lavas and DVP lavas that assimilated lithospheric material. With regards to the two endmember models previously proposed for W isotope anomalies in mantle plumes, neither core-derived W nor an ancient silicate component with anomalous ¹⁸²W can be completely ruled out at this stage. However, due to the covariation of Pb and W isotopes and lower W/Th ratios in asthenosphere-derived DVP lavas, we currently favour a recycled mafic restite component of Hadean age as a source for the 182W deficits in the Deccan-La Réunion plume.

1. Introduction

Short-lived decay systems, especially 182 Hf- 182 W ($t_{1/2} \sim 8.9$ Ma; Vockenhuber et al., 2004) and 146 Sm- 142 Nd ($t_{1/2} \sim 92$ to 103 Ma; Chiera et al., 2024; Friedman et al., 1966), provide important vestiges of processes that occurred during the early formation of the solar system and the Earth. As measurement protocols became more advanced, it is now possible to resolve variations of 182 W and 142 Nd of around 3 to 4 ppm (e. g., Bennett et al., 2007; Caro et al., 2006; Hasenstab-Dübeler et al., 2022;

Mundl et al., 2017; Peters et al., 2018; Saji et al., 2016; Tusch et al., 2022; Willbold et al., 2011).

While the majority of modern igneous rocks do not exhibit resolvable $\mu^{182}W$ or $\mu^{142}Nd$ anomalies (ppm deviations from a terrestrial reference material; e.g., Andreasen et al., 2008; Cipriani et al., 2011; Jansen et al., 2022; Peters et al., 2024; Willbold et al., 2011), some ocean island basalts (OIBs) and continental flood basalts related to deep-rooted mantle plumes exhibit negative $\mu^{182}W$ anomalies (e.g., Jansen et al., 2022; Mundl et al., 2017; Mundl-Petermeier et al., 2019; Peters et al., 2021;

E-mail address: jpakull1@uni-koeln.de (J.J. Pakulla).

https://doi.org/10.1016/j.epsl.2025.119225

^{*} Corresponding author.

Rizo et al., 2019). In the case of the Deccan-La Réunion and Samoa plumes, resolvable $\mu^{142}Nd$ variations were also observed (Horan et al., 2018; Peters et al., 2018, 2021). Global correlations of ³He/⁴He with $\mu^{182}W$ and apparent local correlations with $\mu^{142}Nd$ such as in OIBs from La Reunion were interpreted to either mirror core-mantle interaction where the core displays ¹⁸²W deficits (e.g., Mundl et al., 2017; Mundl-Petermeier et al., 2019; Rizo et al., 2019) or the incorporation of material in the deep mantle that experienced Hadean silicate differentiation within the first 60 to 500 Myrs after solar system formation (e.g., Peters et al., 2018, 2021; Tusch et al., 2022). Selective diffusion of W from Earth's core (e.g., Yoshino et al., 2020), metal-silicate equilibration (e.g., Humayun, 2011), oxide exsolution (Deng and Du, 2023; Rizo et al., 2019) or metal infiltration into Earth's lowermost mantle (Otsuka and Karato, 2012) are processes that were suggested to incorporate core-derived ¹⁸²W deficits in mantle plume source regions. However, metal infiltration has been suggested to be the least likely due to the lack of an expected general enrichment in highly siderophile elements (HSE) in OIB that also display ¹⁸²W deficits (e.g., Mundl et al., 2017; Walker

Seismically anomalous structures named Large Low Shear Wave Velocity Provinces (LLSVPs) and Ultra Low Velocity Zones (ULVZs) at the core-mantle boundary have been suggested to be reservoirs conserving primordial ${}^{3}\text{He}/{}^{4}\text{He}$, $\mu^{182}\text{W}$, and $\mu^{142}\text{Nd}$ signatures (e.g., Labrosse et al., 2007; Mundl et al., 2017). Alternatively, it was also suggested that primordial residual material from silicate differentiation might survive in the lower to mid-mantle as streaks or "blobs" (e.g., Ballmer et al., 2017). Whether this primordial component is stored at the core-mantle boundary or in the mid-mantle, is still an open question. This issue might be resolved by investigating the spatio-temporal evolution of $\mu^{182}W$ and $\mu^{142}Nd$ for single mantle plume systems that have been suggested to potentially entrain such primordial materials at different proportions through their lifetime (e.g., Jones et al., 2019; Williams et al., 2015). Detailed investigation of a single mantle plume throughout its eruptive stages (e.g., plume head to tail) might therefore provide comprehensive information on how primordial components are entrained into mantle plumes (e.g., Jones et al., 2019; Williams et al., 2015), as well as the formation of the primordial components itself. Two previous studies by Mundl-Petermeier et al. (2019) and Peters et al. (2021) that investigated the Iceland plume and the Deccan-La Réunion plume, respectively, indicated that a plume head and tail can tap the

same primordial component (Peters et al., 2021), albeit that appears not always to be the case (e.g., Jansen et al., 2022; Mundl-Petermeier et al., 2019). In contrast, combining information from separate ocean island basalt suites may distort interpretations on the origin of the μ^{182} W and μ^{142} Nd anomalies, since not all plume systems are necessarily affected by the same primordial components (e.g., Jackson et al., 2020). As an additional problem, voluminous melts from plume heads that can lead to the eruption of Large Igneous Provinces are often affected by assimilation of crustal and lithospheric mantle components (e.g., Basu et al., 2020; Hoyer et al., 2023; Pakulla et al., 2023; Peng et al., 1994), thus requiring a more detailed investigation of the effect of assimilation concerning μ^{182} W and μ^{142} Nd compositions.

To assess the evolution of a mantle plume from head to tail, we investigated basaltic samples from the ca. 66 Ma Deccan Volcanic Province (DVP) for their $\mu^{182}W$ and $\mu^{142}Nd$ compositions. The DVP taps the plume head of the well-studied La Réunion OIBs of Quaternary age (e.g., Jansen et al., 2022; Peters et al., 2018, 2021; Rizo et al., 2019). Additionally, we provide new $\mu^{142}Nd$ and Pb isotope data for samples from La Réunion that have been previously investigated for $\mu^{182}W$ (Jansen et al., 2022). Using the newly acquired data we can provide new information on the spatio-temporal evolution of the Deccan-La Réunion plume and its primordial component in the deep mantle.

2. Geological Background

The Deccan Volcanic Province (DVP) is located in central-western India and covers roughly 500,000 km² on a basement including four Archean Cratons (Fig. 1). The volcanic eruption was most likely triggered by the ascending La Réunion plume that connected with the Indian lithosphere possibly as early as 70 Ma (Srivastava et al., 2020). This event caused delamination of the Indian lithospheric mantle (Paul and Ghosh, 2021; Sharma et al., 2018) and dispersed lithospheric mantle and plume material across the Indian upper mantle (Bredow et al., 2017; Paul and Ghosh, 2021). While magmatic processes persisted until approximately 63 Ma (Sheth and Pande, 2014), the major eruptive phase of the DVP took only around one million years from 66.5 to 65.5 Ma (e.g., Schoene et al., 2019). The eruption might have taken place in three to four magmatic pulses (e.g., Schoene et al., 2019), potentially via a multi-magma chamber system (Mittal et al., 2021; Pakulla et al., 2023). Trace element and isotope studies further stress the influence of

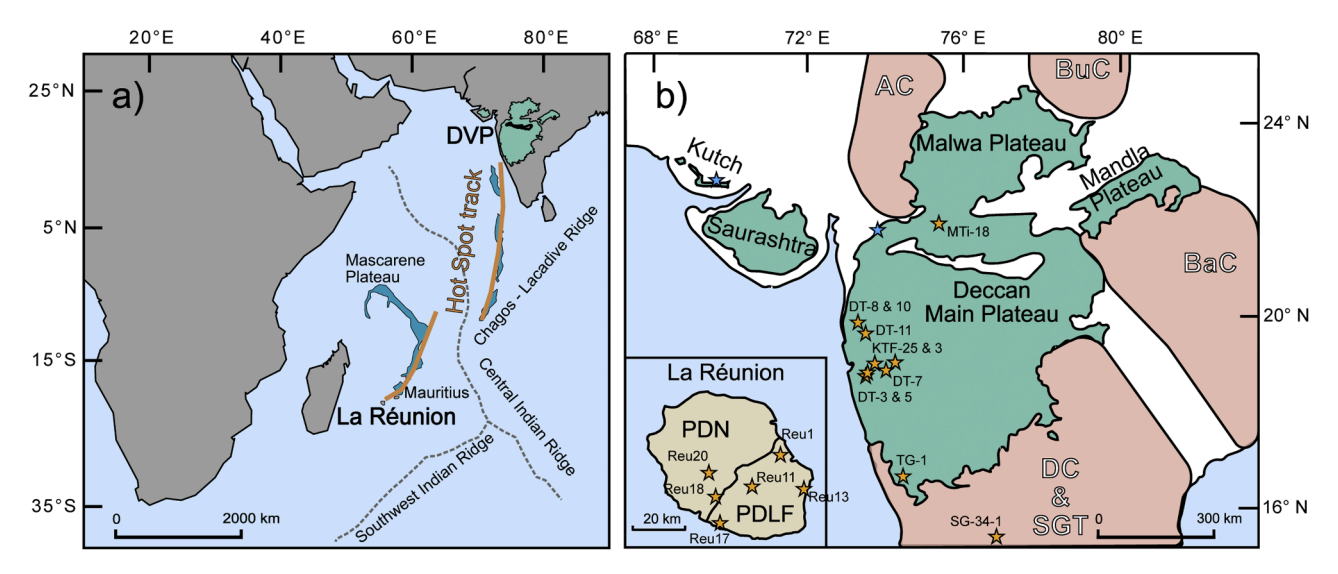


Fig. 1. a) Map of the Indian Ocean showing the relative distance between La Réunion and the DVP. The suggested Hot Spot track, ocean floor plateaus, and ridges were added for reference following White and McKenzie (1989). b) Map of India and La Réunion depicting the Archean cratons, the extent of the DVP, and the approximate sample locations for this study (orange stars) and DVP samples from Peters et al. (2021) (blue stars). The figure was modified from Pakulla et al. (2023). Abbreviations are DC & SGT: Dharwar Craton and Southern Granulite Terrane, BaC: Bastar Craton, AC: Aravalli Craton, BuC: Bundelkhand Craton, PDN: Piton de Neige, PDLF: Piton de la Fournaise.

the La Réunion plume in the generation of the DVP lavas and have indicated a significant contribution of ascending lower mantle material to the formation of the flood basalts (Basu et al., 2020; Pakulla et al., 2023; Peng et al., 1994; Peters et al., 2021; Peters and Day, 2017). A primary DVP melt fed by significant amounts of such lower mantle material evolved to the chemical compositions of the lava flow formations observed today by assimilation of crustal and lithospheric mantle materials (e.g., Basu et al., 2020; Cox and Hawkesworth, 1985; Peng et al., 1994). The resulting geochemical variations including ⁸⁷Sr/⁸⁶Sr, $^{143}\mathrm{Nd}/^{144}\mathrm{Nd},$ and Pb isotopes, as well as major and trace element abundances led to the distinction of 12 chemostratigraphic formations along the stratigraphy of the volcanic succession (e.g., Cox and Hawkesworth, 1985; Suppl. fig. 2). In that sense, the Ambenali formation is typically suggested to display the least contaminated endmember, while the Bushe formation with radiogenic Sr and unradiogenic Nd isotope compositions was explained to have assimilated crustal and lithospheric mantle material (Basu et al., 2020; Cox and Hawkesworth, 1985; Peng et al., 1994). Chemical variations that are intermediate in composition between the Bushe and Ambenali formations typically characterize the other DVP formations indicating the admixture of variable amounts of distinct crustal and lithospheric mantle components (e.g., Basu et al., 2020; Peng et al., 1994). It is speculated that the admixture of wall rock material governs the chemical variations of the DVP lava flows and was inherited during the magma chamber stage (e.g., Cox and Hawkesworth, 1985; Hoyer et al., 2023), whereas others suggest that the chemical compositions might be rather explained by mixing prior to a magma chamber stage either in the plume source or during melt ascent through the lithospheric mantle (e.g., Basu et al., 2020; Pakulla et al., 2023).

3. Samples and methods

In total, 17 samples were investigated in this study for their $^{182} \text{W}/^{184} \text{W}, ^{142,143} \text{Nd}/^{144} \text{Nd},$ and partially for their Pb isotope compositions. Out of these, 6 samples from La Réunion were previously analyzed for ¹⁸²W/¹⁸⁴W and ¹⁷⁶Hf/¹⁷⁷Hf (Jansen et al., 2022). Four samples from the Piton de La Fournaise volcano and two additional samples from the Piton de Neiges volcanic edifice were analyzed (Fig. 1). Most of the samples from the DVP were sampled in close spatial proximity to the Western Ghats Escarpment, whereas sample MTi-18 originated from the Northern DVP south of Mhow (see Pakulla et al., 2023 for more information; Fig. 1). The studied samples belong to the Jawhar, Neral, Bushe, Poladpur, Ambenali, Mahabaleshwar, and Desur formations, respectively (Suppl. fig. 2). The investigated samples therefore cover almost the whole eruptive cycle of the DVP. Additionally, one tonalite-trondhjemite-granodiorite (TTG) suite sample from the Dharwar Craton with an age of \sim 3.4 Ga (SG 34.1; Ravindran et al., 2023) was investigated for its $\mu^{182}W$, $\mu^{142}Nd$, and $^{143}Nd/^{144}Nd$ compositions as well as its trace element abundances. Moreover, previously reported trace element, ⁸⁷Sr/⁸⁶Sr, ¹⁴³Nd/¹⁴⁴Nd, ¹⁷⁶Hf/¹⁷⁷Hf, and ^{206,207}, ²⁰⁸Pb/²⁰⁴Pb data for the DVP, La Réunion, and TTG samples by Jansen et al. (2022; and references therein), Ravindran et al. (2023), and Pakulla et al. (2023) were considered for this study.

According to Pakulla et al. (2023), the DVP samples can be assigned to three distinct magmatic differentiation trends namely, the Group 1 to 3 differentiation trends. Samples studied here correspond to the Group 2 and Group 3 trends which we will refer to throughout the manuscript (Table 1). The Group 2 differentiation trend (Table 1) was suggested to be derived from a La Réunion-like melt or upper mantle melt that assimilated metasomatized lithospheric mantle and, to a lesser extent, crustal material (Pakulla et al., 2023). The Group 3 differentiation trend (Table 1) displays asthenosphere-like trace element and isotope compositions (Pakulla et al., 2023). For Group 3, the mixing of upper mantle-derived melts and plume melts was previously suggested (Pakulla et al., 2023). Samples of Group 1, which were not studied for ¹⁸²W and ¹⁴²Nd due to lack of sufficient sample material, were explained to have incorporated significant amounts of crustal and lithospheric

Lable 1 $\mu^{142} Nd$ for samples investigated in this stuc

=

Sample	Stratigraphy	Group	Group μ^{142} Nd $(8/4)^{\alpha} \pm 95 \%$ CI μ^{14}	\pm 95 % CI	μ^{14} Nd (6/4) ^a	$^{\alpha}$ \pm 95 % CI	$\mu^{182}W(6/4)^{\beta}\pm95\%$ CI $\mu^{183}W(6/4)^{\beta}\pm95\%$ CI $\mu^{182}W(6/3)^{\beta}\pm95\%$ CI	± 95 % CI	(μ ¹⁸³ W (6/4)	± 95 % CI	$\mu^{182}W(6/3)$	$^{\rm p}~\pm~95~\%~{ m CI}$	$\mu^{184}W(6/3)^{\beta}$	± 95 % CI	μ ¹⁸² Wcorr (6/3) ^p	± 95 % CI
Reu-1	PDLF		0.1	3.1	-0.8	3.2	-3.8	3.8	-1.9	4.2	-3.5	2.9	1.3	2.8	-5.3	3.6
Reu-11**	PDLF 1961		9.0-	3.3	-1.6	3.2	-6.1	4.2	-0.9	4.0	-4.8	2.8	9.0	2.7	-5.4	3.8
Reu-11 dup			-0.4	2.2	1.9	4.9										
Reu-13**	PDLF 2002		1.1	2.0	0.5	2.8	-8.8	4.1	-1.2	3.7	-7.7	2.3	0.8	2.5	-8.0	3.6
Reu-17**	PDLF		0.2	1.0	-0.1	2.3	-5.7	2.4	-3.0	3.1	-4.4	2.0	2.0	2.1	2.0	2.1
Reu-18**	PDN, flow		0.0	2.1	0.0	2.5	-1.9	4.5	1.5	4.6	-2.7	3.1	-1.0	3.1	-2.3	4.5
Reu-20**	PDN dike		2.7	2.4	1.9	3.1	0.0	6.3	-3.5	7.5	0.9	4.2	2.3	5.0	-3.6	6.6
Reu-20 dup			1.1	2.8	-0.2	7.3										
DT-10	no formation	2	0.4	3.2	-0.4	3.8	-0.6	2.4	1.8	2.0	-2.9	3.0	-1.2	1.3	-0.6	2.2
DT-8	Jawhar fm.	2	2.9	3.0	2.3	3.7	9.9-	1.8	-2.0	2.4	-2.5	2.6	1.3	1.6	-5.0	1.9
DT-8 dup			2.2	2.6	1.6	3.0										
DT-11	Neral fm.	2	0.0	4.0	-1.1	4.0	-6.3	3.4	-4.3	3.2	-2.9	5.0	2.8	2.1	-8.5	4.5
DT-11 dup			0.0	1.7	2.1	2.2										
KTF-3	Bushe fm.	2	-0.3	3.0	-0.8	3.5	-3.6	2.8	0.1	3.1	-5.7	3.3	0.0	2.1	-5.6	4.0
DT-7	Poladpur fm.	2	-0.1	2.7	9.0	2.9	-4.1	2.2	1.4	2.4	-5.7	2.7	-1.0	1.6	-3.8	2.7
MTi-18	formation unassigned	s p	-0.2	1.5	0.8	3.5	-11.4	3.4	1.3	3.6	-12.7	4.4	-0.9	2.4	-11.0	3.3
KTF-25	Ambenali fm.	3	-1.5	2.1	0.3	2.2	-10.2	4.1	1.7	4.3	-13.2	5.4	-1.1	2.8	-11.1	6.1
DT-3	Ambenali fm.	3	-0.5	2.9	-0.1	2.7	9.9-	3.5	-0.1	2.7	-7.3	2.9	0.1	1.8	-7.4	4.6
DT-3 dup			8.0	2.4	1.7	3.3										
DT-5	Mahabaleshwar fm.	3	-0.5	2.3	-2.1	2.7	-10.1	2.8	0.7	2.5	-10.1	3.0	-0.5	1.7	-9.1	3.1
TG-1	Desur fm.	3	-1.4	2.2	-2.7	3.6	-12.0	2.3	0.7	3.0	-12.6	2.5	-0.5	2.0	-11.6	2.7
SG 34.1	Dharwar TTG		0.3	2.0	-0.2	2.4	2.2	6.2	-1.8	5.9	0.3	9.4	1.2	3.9	-2.0	2.0

 $\mu^{182}W$ (6/4) and $\mu^{183}W$ (6/4) normalized to $^{186}W^{184}W = 0.92767$; $\mu^{182}W$ (6/3) and $\mu^{184}W$ (6/3) normalized to $^{186}W^{183}W = 1.9859$; $\mu^{182}W = [((^{182}W^{184}W)_{sample}/(^{182}W)_{184}W)_{NIST}) - 1]*10^6$.

3

mantle components due to radiogenic Sr and Pb isotope compositions and unradiogenic Nd and Hf compositions in combination with upper crust-like trace element patterns (i.e. enrichment in incompatible elements and negative Nb-Ta anomalies; Pakulla et al., 2023).

Isotope measurements were conducted at the University of Cologne using a Thermo Fisher® Neptune© Plus Multicollector ICP-MS (MC-ICP-MS). More detailed information on digestion, chemical separation, and measurement procedure can be found in Tusch et al. (2019; 2021; 2022) for ¹⁸²W, Hasenstab-Dübeler et al. (2022) for ¹⁴²Nd and ¹⁴³Nd, and Schuth et al. (2011) for Pb isotopes, as well as in the supplements. For $\mu^{142} Nd$, we modified the previous protocol in obtaining very high Nd yields of >99.5 % during the Eichrom© LN Spec resin step to prevent any mass-dependent Nd isotope fractionation that could affect measured u¹⁴²Nd compositions (Garçon et al., 2018; Hasenstab-Dübeler et al., 2022; Saji et al., 2016; Wang and Carlson, 2022). This modification, however, also leads to a poorer Pr-Nd separation compared to that in the original protocol of Hasenstab-Dübeler et al. (2022). To eliminate any potential effects caused by ¹⁴¹PrH⁺, we therefore have additionally doped individual JNdi-1 splits to match the Pr/Nd ratio of each sample (Saji et al., 2016). For mass-bias correction of μ^{142} Nd and μ^{143} Nd/ μ^{144} Nd, we used the exponential law and a ¹⁴⁸Nd/¹⁴⁴Nd ratio of 0.241578 and for $\mu^{182}W$ we used the $^{186}W/^{184}W$ ratio of 0.92767. Ratios of $^{143}\mathrm{Nd}/^{144}\mathrm{Nd}$ have been measured simultaneously during the ¹⁴²Nd/¹⁴⁴Nd sessions and are given relative to a ¹⁴³Nd/¹⁴⁴Nd value of 0.511859 for La Jolla (Lugmair and Carlson, 1978) which is equivalent to a ¹⁴³Nd/¹⁴⁴Nd of 0.512115 for the JNdi-1 (Tanaka et al., 2000).

4. Results

The results of our high-precision measurements are shown in Tables 1 and 2. More details on our $\mu^{182}W$ and $\mu^{142}Nd$ measurements can also be found in the supplements. In short, measurements of $\mu^{182}W$ for two in-house reference samples (160245 and AGC-351) are well within the range of previously reported values (Tusch et al., 2022). We recalculated the external reproducibility with data for the AGC-351 from Tusch et al. (2022) that were prepared on the same instrument using the same analytical protocol, which now results in a long-term average of μ^{182} W of -0.6 ± 2.1 (2 s.d., n = 30). For μ^{142} Nd measurements, our in-house reference material LP-1 has been used and displays $\mu^{142}Nd$ values ($\mu^{142}Nd=0.4\pm2.1$ and -1.8 ± 1.9) identical within error to previously reported data (μ^{142} Nd = 0.4 \pm 1.4, 2 s.d., n = 23, Hasenstab-Dübeler et al., 2022). Additionally, the sample AGC-351 was also measured repeatedly for its $\mu^{142}Nd$ composition and resulted in a long-term value of -1.8 ± 2.5 (2 s.d., n = 15). This sample is now well characterized and can serve as an additional in-house reference material in future studies.

In contrast to previous studies from Peters et al. (2018, 2021) we do not find resolvable μ^{142} Nd anomalies in samples from the DVP (μ^{142} Nd = 0.1 \pm 0.8, 95 % CI, n = 13) as well as La Réunion (μ^{142} Nd = 0.5 \pm 0.8, 95 % CI. n = 8) (Fig. 2). The studied TTG sample SG-34.1 from the Dharwar Craton also does not display a resolvable $\mu^{142}Nd$ anomaly (Table 1). The 143 Nd/ 144 Nd compositions acquired during the measurement of μ^{142} Nd are consistent with previously measured, 146Nd/144Nd-normalized values for the same samples by Pakulla et al. (2023). In contrast to μ^{142} Nd, we find negative μ^{182} W anomalies as low as -12.0 ± 2.3 (TG-1; Desur fm.). These $\mu^{182}W$ values overlap with previously reported $\mu^{182}W$ values for volcanic rocks from La Réunion ($-4.9 \pm 1.5, 95 \%$ CI, n = 18; Peters et al., 2021; Jansen et al., 2022), but expand the compositional spectrum towards larger ¹⁸²W deficits. Interestingly, samples from the distinct DVP groups also display distinct $\mu^{182}W$ values, with lithosphere-derived Group 2 having an average of -4.2 ± 3.0 (95 % CI, n = 5) and asthenosphere-derived Group 3 having an average of -10.1 \pm 2.6 (95 % CI, n=5), the latter being distinctively lower than the La Réunion average ($-4.9 \pm 1.5, 95 \% \text{ CI}$; n = 14; Fig. 2, Suppl. fig. 1). The Archean TTG SG-34.1, however, does not display a resolvable µ¹⁸²W anomaly (Table 1). We do not identify a correlation of $\mu^{182}W$ with

Cong-lived radiogenic isotopes, W, and Th concentration data of samples investigated in this study. Tungsten, Th, and 176Hf/177H for La Réunion samples (Reu) from Jansen et al. (2022). Isotope data (except 143Nd/144Nd) the Archean TTG from the Dharwar Craton (SG 34-1) are from Ravindran et al. (2023). Isotope and trace element data (except ¹⁴³Nd/¹⁴⁴Nd) for Deccan samples are from Pakulla et al. (2023). Δ^{207} Pb/²⁰⁶pb was

Sample Stratigraphy Reu-1 PDLF Reu-11 PDLF 1961									
1	Group	[g/gu] tT dr	W [ug/g]	W/Th	$^{176}{ m Hf}/^{177}{ m Hf}$	¹⁴³ Nd/ ¹⁴⁴ Nd	$^{206}{ m pb}/^{204}{ m pb}$	$^{207}{ m Pb}/^{204}{ m Pb}$	ΔPb 7/6
		2.56	0.363	0.142	0.283041 ± 0.000006	0.512858 ± 0.000002	18.908 ± 0.001	15.602 ± 0.001	6.1
		2.57	0.331	0.129	0.283048 ± 0.000005	0.512866 ± 0.000002	18.971 ± 0.001	15.609 ± 0.001	6.2
Reu-11 dup						0.512867 ± 0.000003			
Reu-13 PDLF 2002		2.11	0.281	0.133	0.283040 ± 0.000005	0.512865 ± 0.000003	18.894 ± 0.001	15.607 ± 0.001	8.9
Reu-17 PDLF		2.65	0.308	0.116	0.283038 ± 0.000005	0.512852 ± 0.000002	18.925 ± 0.001	15.606 ± 0.001	6.4
Reu-18 PDN, flow		2.01	0.225	0.112	0.283044 ± 0.000006	0.512859 ± 0.000002	18.974 ± 0.001	15.612 ± 0.001	6.4
Reu-20 PDN dike		1.30	0.155	0.119	0.283047 ± 0.000004	0.512867 ± 0.000002	18.950 ± 0.001	15.610 ± 0.001	6.5
Reu-20 dup						0.512868 ± 0.000008			
DT-10 formation unassigned	signed 2	3.22	0.261	0.081	0.282935 ± 0.000006	0.512634 ± 0.000002	19.802 ± 0.009	15.760 ± 0.010	12.2
DT-8 Jawhar fm.	2	4.07	0.272	0.0669	0.282765 ± 0.000007	0.512432 ± 0.000002	19.685 ± 0.010	15.776 ± 0.012	15.1
DT-8 dup						0.512432 ± 0.000003			
DT-11 Neral fm.	2	2.71	0.145	0.0533	0.282558 ± 0.000007	0.512263 ± 0.000003	19.794 ± 0.010	15.826 ± 0.011	18.9
DT-11 dup						0.512263 ± 0.000002			
KTF-3 Bushe fm.	2	1.84	0.0835	0.0453	0.282970 ± 0.000005	0.512680 ± 0.000002	18.519 ± 0.001	15.581 ± 0.001	8.3
DT-7 Poladpur fm.	2	1.99	0.179	0.0904	0.282984 ± 0.000007	0.512703 ± 0.000003	19.200 ± 0.009	15.674 ± 0.012	10.2
	signed 3	1.94	0.218	0.113	0.283049 ± 0.000008	0.512797 ± 0.000001	17.701 ± 0.010	15.398 ± 0.013	-1.2
KTF-25 Ambenali fm.	3	1.34	0.116	0.0867		0.512867 ± 0.000003	18.085 ± 0.002	15.478 ± 0.002	2.7
DT-3 Ambenali fm.	3	1.97	0.211	0.107	0.283044 ± 0.000007	0.512775 ± 0.000003	17.637 ± 0.008	15.400 ± 0.010	-0.3
DT-3 dup						0.512775 ± 0.000002			
DT-5 Mahabaleshwar fm.	r fm. 3	1.48	0.149	0.101		0.512694 ± 0.000003	17.255 ± 0.007	15.352 ± 0.009	-0.9
TG-1 Desur fm.	3	2.42	0.293	0.121		0.512816 ± 0.000002	17.971 ± 0.009	15.448 ± 0.012	6.0
SG 34.1 Dharwar TTG		10.3	0.270	0.0262	0.281143 ± 0.000004	0.510492 ± 0.000002	20.662 ± 0.0006	18.331 ± 0.001	260

Table 3Trace element and isotope compositions of the modeling endmembers for Fig. 3.

	Indian crust (TTG)	La Réunion melt	Deccan endmember melt
Nb [μg/g]	13.9	18.2	18.2
Th [μg/g]	10.3	1.90	1.90
Pb [μg/g]	8.70	1.27	1.27
Nd [μg/g]	28.1	22.2	22.2
W [μg/g]	0.270	0.220	0.220
Nb/Th	1.35	9.58	9.58
ε^{143} Nd	-58	8.7	8.7
206 Pb/ 204 Pb	20.662	18.921	16.5
207 Pb/ 204 Pb	18.331	15.585	15.25
Δ^{207} Pb/ 206 Pb	260	4.35	-2.96
$\mu^{182}W$	2.2	-4.9	-11.0

 $\mu^{142}Nd$ in La Réunion samples in contrast to a previous study by Peters et al. (2021) (Suppl. fig. 3).

Lead isotope data of La Réunion samples range in $^{206}\text{Pb}/^{204}\text{Pb}$ from 18.894 ± 0.001 to 18.974 ± 0.001 , in $^{207}\text{Pb}/^{204}\text{Pb}$ from 15.603 ± 0.001 to 15.612 ± 0.001 , and in $^{208}\text{Pb}/^{204}\text{Pb}$ from 39.024 ± 0.002 to 39.090 ± 0.002 and overlap with previously reported values (cf. Bosch et al., 2008).

5. Discussion

5.1. Deep mantle sources and involvement of lithospheric mantle

The combination of trace element and isotope systematics can discriminate between source signatures from the asthenospheric mantle, the lithospheric mantle, and crustal assimilation during ascent. In this

regard, canonical trace element ratios (e.g., Nb/Th, Nb/Ta, Ce/Pb; Nb/ Th $\sim 15.5 \pm 4.5$ calculated from ridge basalts in Jenner and O'Neill, 2012) are particularly powerful, since these are not affected by the degree of melting or fractional crystallization but only change due to the involvement of lithospheric mantle and crust (e.g., Hofmann et al., 1986, 2022; Jansen et al., 2024; Pakulla et al., 2023; Pfänder et al., 2007). In case of the DVP, where many volcanic rocks (but not all) fall into the compositional fields of mantle-derived rocks based on long-lived radiogenic isotopes (e.g., Basu et al., 2020; Hoyer et al., 2023; Pakulla et al., 2023), their diagnostic trace element compositions (e.g., Nb/Th, Th/Ta, Nb/Zr) show strong differences (e.g., Basu et al., 2020; Hoyer et al., 2023; Pakulla et al., 2023; Peng et al., 1994, 1998). In this regard, Pakulla et al. (2023) distinguished the DVP lava flows based on their diagnostic trace element compositions into three groups. Group 1 marks samples with low Nb/Th and enriched radiogenic isotope compositions, unlike groups 2 and 3 (Pakulla et al., 2023). Amongst these, Group 2 samples display lower Nb/Th ratios than Group 3 samples that display higher Nb/Th comparable to La Réunion samples (Fig. 3a). The relative depletion of Nb in Group 1 and 2 samples suggest involvement of crustal or lithospheric mantle components (e.g., Basu et al., 2020; Cox and Hawkesworth, 1985; Hover et al., 2023; Pakulla et al., 2023), whereas the Nb/Th compositions of Group 3 indicate an asthenospheric mantle source comparable to the La Réunion mantle source (Pakulla et al., 2023). The trace element variations are mirrored in their $\mu^{182}W$ values, where Group 3 samples show resolvable larger $^{182}\mathrm{W}$ deficits than Group 2 samples (Fig. 3a). Group 2 samples lie on a mixing array with endmembers defined by Group 3-like trace element and $\mu^{1\bar{8}2}W$ compositions and the composition of Archean crust as represented by an Indian Archean TTG (Fig. 3a). As for Group 2 from the DVP, samples from La Reunion also plot between these two endmembers. Likewise, these

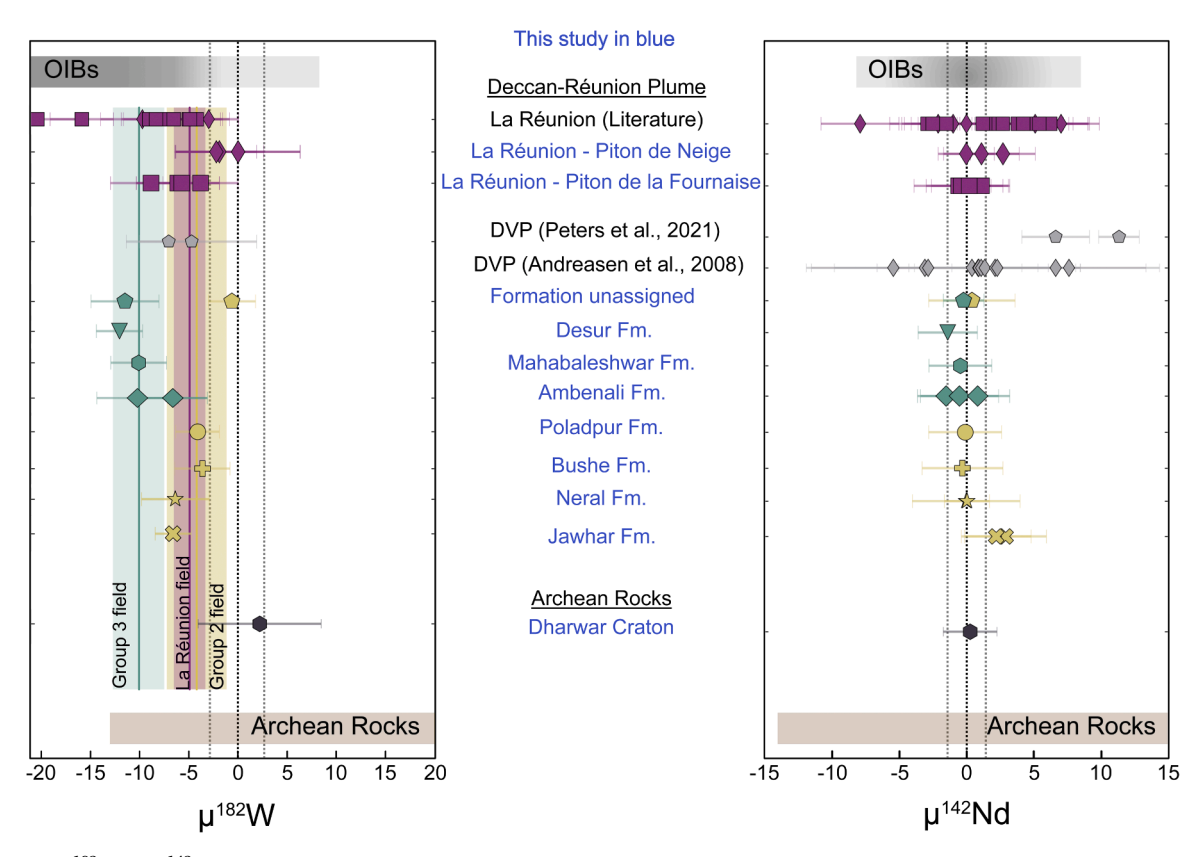


Fig. 2. Measured μ^{182} W and μ^{142} Nd compositions of volcanic rocks from La Réunion and the DVP. Literature data for the DVP and La Réunion are from Andreasen et al. (2008), Peters et al. (2018; 2021), Rizo et al. (2019), and Jansen et al. (2022). Additional, references for the OIB and Archean fields can be found in the supplements. Different DVP chemical groups display unique μ^{182} W compositions that are resolvable from each other. Samples were grouped based on the characterization of Pakulla et al. (2023). There is a resolvable difference in μ^{182} W between DVP Group 3 and La Réunion basalts. μ^{182} W was normalized to μ^{186} W/ μ^{184} W = 0.92767 and μ^{142} Nd to μ^{148} Nd/ μ^{144} Nd = 0.241578. Sample-standard bracketing was applied.

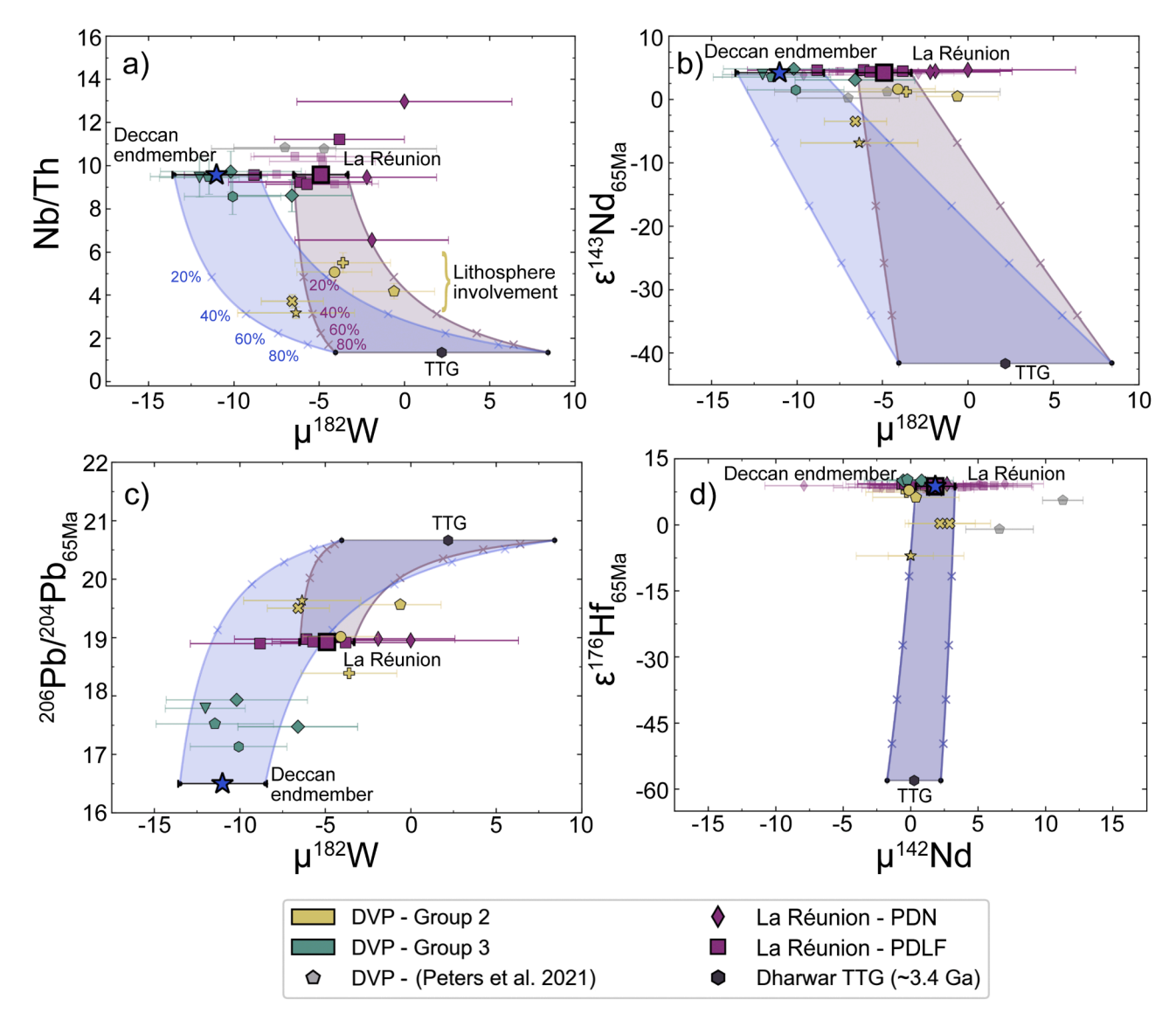


Fig. 3. Mixing models involving a measured Archean TTG, a La Réunion basalt composition, and a Deccan endmember composition (Table 3). Shown here is a simplified legend, for an explanation for each symbol, see Fig. 2 or Suppl. fig. 4. a) Nb/Th and b) ϵ^{143} Nd_{65Ma} vs. μ^{182} W showing that Group 2 samples overlap with mixing arrays between an Archean TTG and a La Réunion-like composition and the Deccan endmember composition with lower μ^{182} W values. Group 3 samples display lower μ^{182} W values than La Réunion volcanics and no indication of significant involvement of crust or lithosphere. c) 206 Pb/ 204 Pb_i vs. μ^{182} W showing that Group 2 basalts can be reproduced by mixing Archean TTG and a La Réunion-like compositions, while Group 3 samples cannot. d) In ϵ^{176} Hf_i vs. μ^{142} Nd space Group 2 samples plot on a mixing array between La Réunion volcanics and an Archean TTG. Literature data is from Jansen et al. (2022) and Peters et al. (2021).

patterns can also be observed in $\mu^{182}W$ - $\epsilon^{143}Nd$ space and $\mu^{182}W$ - $\epsilon^{206}Pb/^{204}Pb$ space (Fig. 3b, c). However, in the latter, Group 3 differs from La Réunion samples in their lower $^{206}Pb/^{204}Pb$ (Fig. 3c, Suppl. fig. 4) and $\Delta^{207}Pb/^{206}Pb$ (Fig. 4) which depicts the offset in $^{207}Pb/^{206}Pb$ between a sample and the northern hemisphere reference line (NHRL; Hart, 1984). In $^{207}Pb/^{204}Pb$ - $^{206}Pb/^{204}Pb$ space, it becomes evident that Group 3 samples partially display lower $^{207}Pb/^{204}Pb$ compositions than La Réunion lavas, making a connection to a "modern" La Réunion mantle source less likely (Suppl. fig. 4). Admixture of an endmember with high $^{207}Pb/^{204}Pb$ - $^{206}Pb/^{204}Pb$ and with $^{182}W \sim 0$ values, possibly represented by Archean crustal and lithospheric mantle material, to the DVP Group 3 source could reproduce the Pb and W isotope compositions of DVP Group 2 and La Réunion lavas (Suppl. fig. 4).

It was previously suggested that the low ²⁰⁶Pb/²⁰⁴Pb of the DVP melts (e.g. Group 3) derived from larger amounts of Indian depleted upper mantle material and minor amounts of lower crustal material potentially amphibolitic or granulitic in compositions (e.g., Hoyer et al., 2023; Pakulla et al., 2023). However, considering combined Pb, Nd, and

W isotope compositions, such a crustal component in the source of Group 3 seems unlikely. Typical crustal rocks observed in the Dharwar Craton basement that is covered by DVP lavas are TTGs and gneisses which display high $^{207}\text{Pb}/^{204}\text{Pb}$ and $^{206}\text{Pb}/^{204}\text{Pb}$, low $\epsilon^{143}\text{Nd},$ and apparently no $\mu^{182}\text{W}$ anomalies (Ravindran et al., 2023; Meen et al., 1992; Fig. 3, Suppl. fig. 4). These characteristics, however, are not observed in DVP Group 3 samples which display negative $\mu^{182}\text{W}$ values and low $^{206}\text{Pb}/^{204}\text{Pb}$ ratios (Fig. 2, 4).

The Indian upper mantle, however, displays unradiogenic $^{206}\text{Pb/}^{204}\text{Pb}$ ratios and slightly elevated $\Delta^{207}\text{Pb/}^{206}\text{Pb}$ values compared to other upper mantle-derived rocks (Dupal anomaly; Dupré and Allègre, 1983; Hart, 1984). While it might be possible that portions of the upper mantle may have inherited anomalous ^{182}W signatures, recent studies rather indicate that the depleted upper mantle does not display anomalous $\mu^{182}\text{W}$ compositions (Jansen et al., 2022; Peters et al., 2024). So far only one sample from the Indian upper mantle has been studied for ^{182}W and it does not display a resolvable anomaly ($\mu^{182}\text{W}=3.5\pm3.5$; Mundl et al., 2017). Thus, assuming $\mu^{182}\text{W}\sim0$ for the depleted

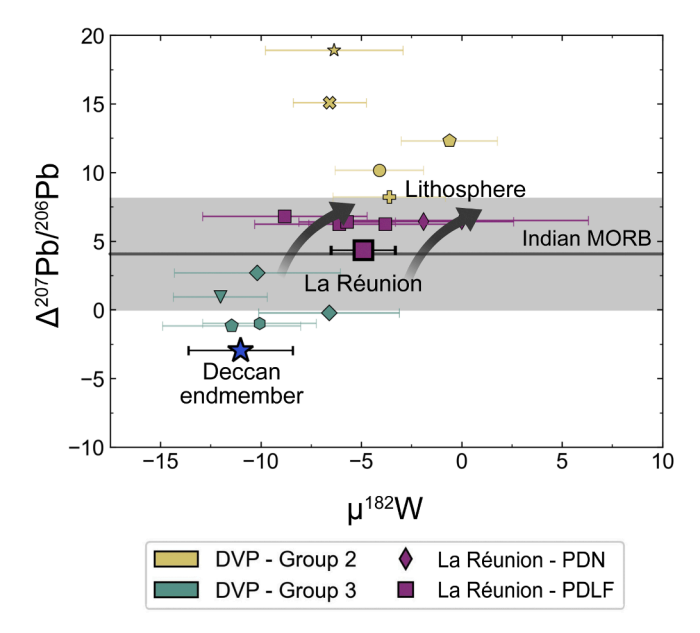


Fig. 4. Plot of $\Delta^{207} Pb/^{206} Pb$ (following Hart, 1984) vs $\mu^{182} W$ indicating that DVP basalts of Group 3 have a low $\Delta^{207} Pb/^{206} Pb$ which plot at the lower end expected from Indian MORB (Mid Ocean Ridge Basalt from PetDB - https://search.earthchem.org/ for more information see supplements). Shown here is a simplified legend, for an explanation of each symbol, see Fig. 2 or Suppl. fig 4. The average La Réunion Pb-composition (Bosch et al., 2008) overlaps with the Indian MORB average. A mixture of the Deccan endmember (Table 3) with lower $\mu^{182} W$ and delaminated Indian lithosphere in different proportions can potentially replicate the isotope composition of La Réunion melts. Group 2 samples have higher $\Delta^{207} Pb/^{206} Pb$ than Indian MORB consistent with further involvement of lithosphere and crust.

upper mantle, admixing upper mantle material to the La Réunion source could explain the lower $^{206}\text{Pb}/^{204}\text{Pb}$ compositions of Group 3 melts, but this cannot explain their more negative $\mu^{182}W$. On the contrary, the addition of upper mantle material to the Group 3 source could explain La Réunion $\mu^{182}W$ values but fails to explain the more radiogenic Pb isotope compositions of La Réunion basalts compared to Group 3 and Indian MORB (Suppl. fig. 4; cf. Bosch et al., 2008). Thus, considering that the basalts from DVP and La Reunion tap a comparable mantle source, the admixture of upper mantle material alone likely fails to explain the composition of both groups.

5.2. Temporal evolution of ^{142}Nd and ^{182}W

Short-lived isotope anomalies in mantle plumes can mirror the entrainment of primordial reservoirs like core material due to coremantle interaction (e.g., Mundl et al., 2017; Rizo et al., 2019), leftovers from early silicate differentiation (e.g., Peters et al., 2018), and ancient recycled crustal components (e.g. Peters et al., 2021; Tusch et al., 2022). As plumes may tap different primordial reservoirs between plume-head and -tail (e.g. Jones et al., 2019) or episodically different reservoirs (Williams et al., 2015), it is possible to identify primordial mantle domains as endmembers of compositional trends. In the case of $\mu^{182}W$ for the Deccan-La Réunion plume, we find resolvable deficits up to -12.0 ± 2.3 (95 % CI) for DVP Group 3 samples, marking one compositional endmember. Interestingly, we also observe that the $\mu^{182}\mbox{W}$ anomalies of DVP groups 2 and 3 are statistically resolvable from each other (Fig. 2). In this regard, Group 2 samples display an average $\mu^{182}W$ value of -4.2 ± 3.0 (95 % CI, n=5) and Group 3 samples an average μ^{182} W value of -10.1 ± 2.6 (95 % CI, n = 5). We interpret this difference as further evidence for distinct parental melts that fed the different geochemical members of the DVP in good agreement with previous suggestions (Melluso et al., 2006; Pakulla et al., 2023). The average

 $\mu^{182} W$ value of DVP Group 3 is also distinguishable from the average μ^{182} W value of La Réunion lavas (-4.9 \pm 1.5, 95 % CI; Peters et al., 2021; Jansen et al., 2022, Fig. 2, Suppl. fig. 1), but DVP Group 2 basalts are indistinguishable from La Réunion basalts. It is important to note that a previous study by Rizo et al. (2019) reported more negative $\mu^{182}W$ anomalies of -15.7 ± 3.2 and -20 ± 5.1 for lapilli from the 2010 and 2014 eruptions on La Réunion. Such negative $\mu^{182}W$ signatures, however, have so far not been identified by other studies for younger lavas erupted in 2001, 2002, and 2007 (Jansen et al., 2022; Peters et al., 2021). These more negative $\mu^{182}W$ signatures may hint toward episodic entrainment of even more primordial material, but this remains speculative. The distinct $\mu^{182}W$ groups are also supported by further statistical modelling and evaluation such as student's t-tests as well as Monte Carlo Bootstrap simulations (see supplements), also when considering data by Rizo et al. (2019). In summary, we propose that the lower u¹⁸²W values of the asthenosphere-derived DVP Group 3 compared to the slightly higher values of primitive La Réunion basalts provide evidence for a change in the incorporation of primordial material into the Deccan-La Réunion plume.

Previously reported µ¹⁴²Nd anomalies for basalts from the Deccan-La Réunion plume were suggested to originate from tapping an isolated source in the mantle that carries a signature of magma ocean differentiation, as indicated by a correlation between $\mu^{142}Nd$ and ${}^{3}He/{}^{4}He$ (Peters et al., 2018). However, recently this view was modified and an apparent trend between $\mu^{142}Nd$ and $\mu^{182}W$ for the same La Réunion samples was taken as evidence for recycled crustal material in the source of the Deccan-La Réunion plume, combined with entrainment of core-derived material deficient in ¹⁸²W (Peters et al., 2021). In our study, we could not identify resolvable $\mu^{142}Nd$ anomalies in the investigated La Réunion and DVP samples, even though the investigated samples span a wide range in $\mu^{1\hat{8}2}W$ values (Fig. 2, Suppl. fig. 3). Whether the discrepancy in $\mu^{142}Nd$ between the different studies reflects an analytical bias or whether lavas on La Reunion show a larger spread in μ^{142} Nd than DVP lavas still needs to be investigated. An argument in favor of the latter view is that Nd isotope data in both studies were reproduced on different sample aliquots.

5.3. The origin of ¹⁸²W deficits in the Deccan-La Réunion plume – core signature or ancient silicate reservoirs?

The origin of ¹⁸²W deficits identified in plume-derived OIBs is still debated. A popular explanation is that core-derived material deficient in ¹⁸²W was admixed to the source of mantle plumes, which are suggested to be rooted in ULVZs and LLSVPs (Mundl et al., 2017; Mundl-Petermeier et al., 2020b; Rizo et al., 2019). Diffusion of W from Earth's core (Yoshino et al., 2020), metal-silicate equilibration (e.g., Humayun, 2011), and oxide exsolution (Deng and Du, 2023; Rizo et al., 2019) are the favored mechanisms that may lead to ¹⁸²W deficits in mantle plumes. A silicate layer on top of Earth's core or exsolved oxides in isotopic equilibrium would also inherit the expected coupled enriched ¹⁸⁷Os/¹⁸⁸Os and ¹⁸⁶Os/¹⁸⁸Os compositions from Earth's core (e.g., Brandon and Walker, 2005). In fact, coupled enrichments in ¹⁸⁷Os/¹⁸⁸Os and ${\rm ^{186}Os/^{188}Os}$ for Gorgona and Hawaii plume melts have been previously suggested to derive from the core (Brandon et al., 1998, 2003), and these lavas also display ¹⁸²W deficits (Mundl et al., 2017; Walker et al., 2023; Willhite et al., 2024). However, when assuming a core-derived origin for Os and W, a correlation between the two isotope systems is expected, but currently not observed (Mundl-Petermeier et al., 2019; Walker et al., 2023; Willhite et al., 2024). Possible explanations for this decoupling may be a more complex evolution of $^{187} \text{Os}/^{188} \text{Os}$ due to additional recycled components (Ireland et al., 2011; Walker et al., 2023) or a lack of core-derived Os (Lassiter, 2006; Luguet et al., 2008). Selective diffusion of W into the lowermost mantle would obviate the need for an Os-W correlation, which is currently used to explain ¹⁸²W deficits in OIBs (e.g., Mundl-Petermeier et al., 2020b; Peters et al., 2021; Yoshino et al., 2020). However, the process of selective

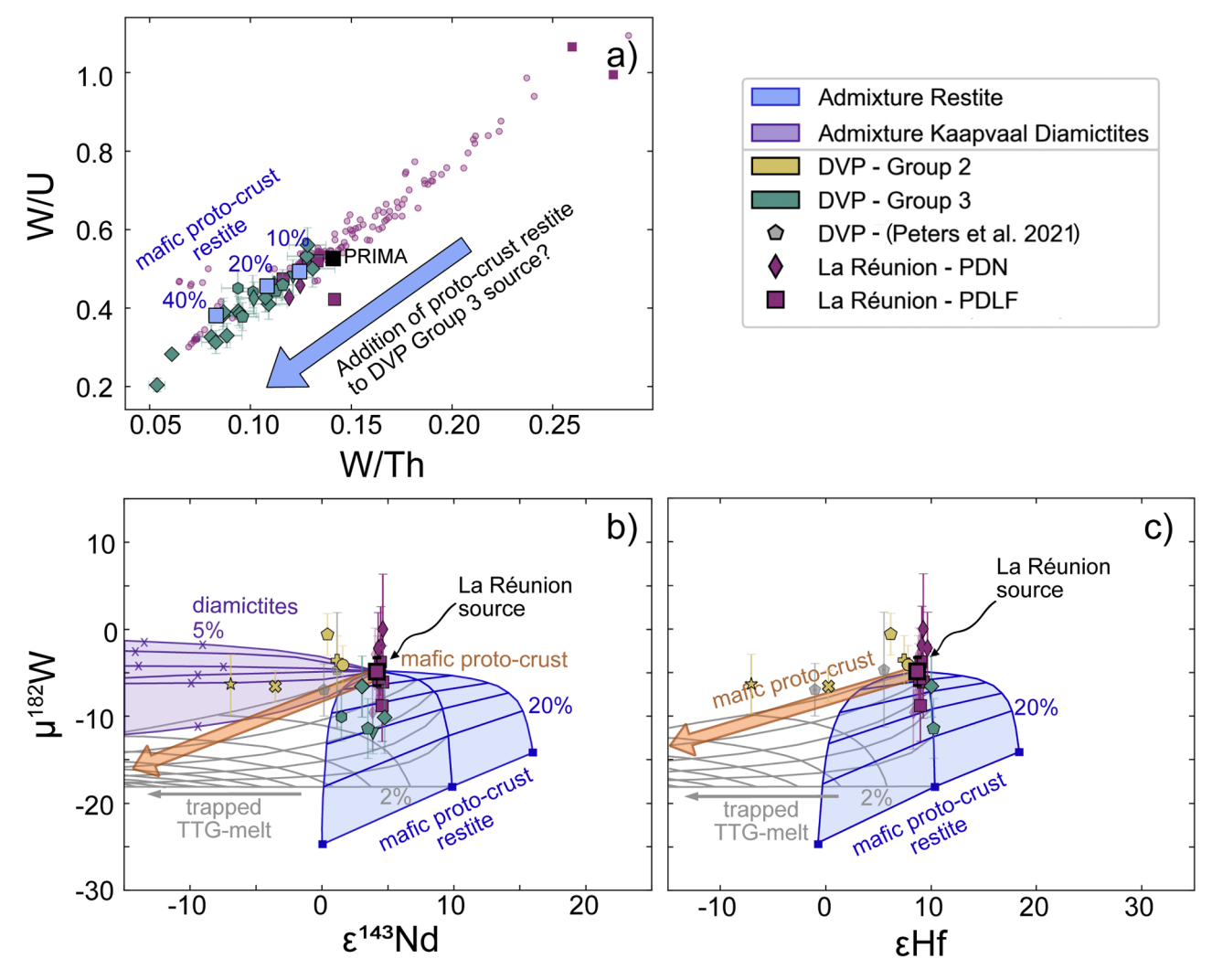


Fig. 5. a) W/U and W/Th compositions of La Réunion melts and DVP Group 3 (data from Pakulla et al., 2023). Bold La Réunion symbols in a) illustrate samples studied in Peters et al. (2021), Jansen et al. (2022), and this study that were also studied for short-lived isotopes. DVP Group 3 melts typically display a slight depletion in W relative to most La Réunion melts. Such systematics can be explained when a mafic proto-crust restite is being admixed to the mantle source (see blue markers; percentage indicates the amount of proto-crust restite admixed to the mantle source). b, c) Mixing models illustrating the mixing of mafic proto-crust restite with the La Réunion mantle source considering a primitive mantle-like trace element and La Réunion-like isotope composition. A 3-component mixing model between the La Réunion source mantle, a mafic restite, and a trapped TTG melt in the restite was added as well. We used the model from Tusch et al. (2022) to model the compositions of the proto-crust formed at 4.35 Ga, the compositions of the restite and trapped TTG melts that formed at 3.55Ga and their respective modern-day isotope compositions. The three different mafic restite endmembers (marked in blue; 20 % mixing steps) correspond to different degrees of melting (10, 15, and 20 %) that produced the mafic proto-crust. We further include mixing calculations with diamicities from the Kaapvaal craton (Mundl et al., 2018 and references therein) as an upper crustal analogue. Crosses along the mixing lines indicate the mixing proportions. Isotope and trace element compositions of DVP Group 3 melts are broadly consistent with the addition of a mafic restite component. Upper crustal material alone as depicted by diamicities cannot reproduce the compositions of DVP Group 3 but are more consistent with DVP Group 2 compositions. Additional mixing plots can be found in the supplements. La Réunion and DVP literature data are from Jansen et al., 2022 and Peters et al., 2021. Mixing endmember compositions are given in the supplemen

grain-boundary diffusion of W at core-mantle boundary conditions was recently challenged by new ab initio calculations (Peng et al., 2024). In that sense, coupled diffusion of primordial high $^3\mathrm{He}/^4\mathrm{He}$ from the core into the lower mantle may indeed explain observed co-variations of $^{182}\mathrm{W}$ and $^3\mathrm{He}/^4\mathrm{He}$ (e.g., Mundl et al., 2017). However, not all OIBs with elevated $^3\mathrm{He}/^4\mathrm{He}$ display $^{182}\mathrm{W}$ deficits (e.g., Herret et al., 2023; Mundl-Petermeier et al., 2020a) and the lack of very high $^3\mathrm{He}/^{22}\mathrm{Ne}$ in OIBs have been suggested to be inconsistent with a derivation of noble gases from Earth's core (Li et al., 2022). The absence of correlations between lithophile elements and $\mu^{182}\mathrm{W}$ has further been used as evidence for a core-derived origin of $^{182}\mathrm{W}$ deficits (Mundl-Petermeier et al., 2019, 2020b; Walker et al., 2023). However, recently Willhite et al. (2024) provided evidence for co-variations of $\mu^{182}\mathrm{W}$ and lithophile elements in the Hawaiian plume which may hint towards a Hadean silicate component in its source. Previously, Tusch et al. (2022) suggested

that a residual mafic proto-crustal restite from the formation of Earth's early felsic crust may explain the ^{182}W deficits in mantle plumes, and such recycled material could indeed produce correlations of lithophile elements with ^{182}W . Such mafic proto-crustal restites may have undergone extraction of felsic melts, leading to delamination and potential storage in the deep mantle. Indeed, ULVZs that may store negative $\mu^{182}\text{W}$ anomalies (cf. Mundl-Petermeier et al., 2019), have been directly connected to recycled material at the core mantle boundary (Su et al., 2024; Wolf et al., 2024). Thus, an origin of ^{182}W deficits from Hadean silicate reservoirs seems highly plausible and needs to be further tested.

In the case of the Deccan-La Réunion plume, the addition of upper crustal material that possesses ¹⁸²W deficits is not suitable to reproduce the short- and long-lived isotope compositions of Group 3. This is shown by mixing models (Fig. 3, 5) with Dharwar Craton basement and glacial diamictites from the Kaapvaal craton (Mundl et al., 2018) that may

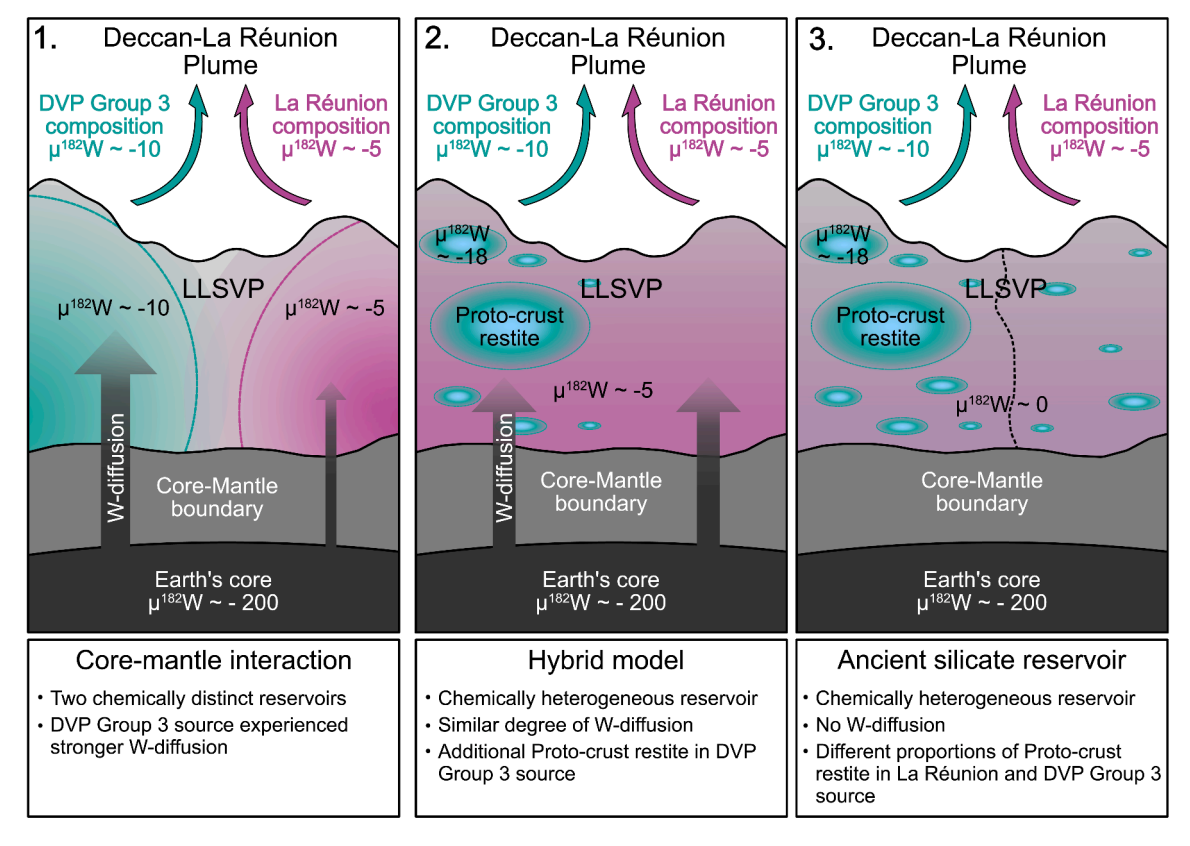


Fig. 6. Model sketch depicting the three possible scenarios discussed in Section 5.3. 1) DVP Group 3 and La Réunion melts originate from chemically distinct reservoirs where the source of DVP Group 3 experienced a higher degree of core-mantle interaction. 2) The La Réunion source is relatively heterogeneous in its composition but was homogeneously affected by core-mantle interaction. Additional incorporation of a mafic proto-crust restite led to the chemical differences between DVP Group 3 and La Réunion melts. 3) The mantle source of the DVP Group 3 and La Réunion was not affected by core-mantle interaction. Chemical differences originate solely from different proportions of mafic proto-crust restite in the source.

represent averaged crustal source materials in the region by the Cretaceous period. The addition of such a crustal material is rather consistent with Group 2 melts which were previously suggested to have incorporated crustal and lithospheric mantle material (Pakulla et al., 2023). Thus, an asthenospheric origin for the distinct ¹⁸²W deficits of DVP Group 3 and La Réunion melts is more likely.

For the Deccan-La Réunion plume, both a core-derived and an early silicate reservoir-derived origin for the ¹⁸²W deficits are plausible. A core-derived origin needs to explain why La Réunion melts with nearly similar trace element and long-lived isotope compositions compared to the most primitive Group 3 melts display resolvable larger $^{182}\mathrm{W}$ deficits. A possible scenario is that two chemically similar reservoirs received distinct amounts of core-derived W deficient in ¹⁸²W via the diffusion of W in the lowermost mantle (e.g., Yoshino et al., 2020). In this case, the mantle source corresponding to Group 3 melts initially had less radiogenic Pb-isotope compositions. Only minor amounts of core-diffused W would be sufficient to affect the ¹⁸²W of the Earth's mantle and thus cannot be identified by an increase in W concentration in the plume melts. Furthermore, DVP melts display similar Os isotope compositions to La Réunion melts but also extend to more radiogenic ¹⁸⁷Os/¹⁸⁸Os which have been attributed to the assimilation of crustal materials (Peters and Day, 2017). Thus, Os is unfortunately not suitable for assessing core contributions to DVP lavas. Concentrations of HSE in DVP lavas are comparable to La Réunion melts and therefore rule out direct assimilation of core metal into the sources of the Deccan-La Réunion plume (Peters and Day, 2017). Helium isotope data are currently still inconclusive, as melts from the DVP either display similar ³He/⁴He compositions as La Réunion melts or lower (Basu et al., 1993; Peters et al., 2017). As of now, no ³He/⁴He isotope measurements have been conducted for DVP samples that can be attributed to Group 3. Future

studies on He and potentially ^{186}Os - ^{187}Os isotope compositions of pristine DVP basalts may be helpful to test if a stronger core contribution in DVP Group 3 relative to La Réunion melts is present. Collectively, a core-derived origin of ^{182}W deficits in DVP lavas is possible but current data of the most pristine DVP lavas do not show chemical differences from La Réunion melts that could be ascribed to core-mantle interaction except for $\mu^{182}\text{W}$.

Tusch et al. (2022) proposed that $\mu^{182}W^{-143}Nd/^{144}Nd$ systematics of a common low $\mu^{182}W$ compositional endmember in OIBs can be reproduced by recycled Hadean mafic proto-crustal restites. Such restites should be devoid of He and depleted in U and Th, and thus do not produce ⁴He in larger amounts by radioactive decay. If recycled into an undegassed mantle source, such a reservoir would virtually not affect the ³He/⁴He budget. However, as outlined in the original model of Tusch et al. (2022) such a proto-crustal restite component may have undergone felsic melt depletion and trapping of such melts could have supplied U-Th and with time, some ingrowth of ⁴He. If mixed into an undegassed mantle portion, the ³He/⁴He ratios may then have been lowered compared to a reservoir unaffected by such a restite component. This mixed component might not be resolved in a global compilation of ¹⁸²W and ${}^{3}\text{He}/{}^{4}\text{He}$ (Suppl. fig. 5), where distinct ${}^{3}\text{He}/{}^{4}\text{He}-\mu^{182}\text{W}$ endmembers were indicated (Jackson et al., 2020), but might be visible in detailed investigations of individual mantle plumes. Indeed, if ³He/⁴He ratios in the pristine Group 3 DVP melts are lower than in La Réunion basalts, as found in some DVP melts (e.g., Basu et al., 1993; Peters et al., 2017), the addition of a recycled restite with somewhat elevated U and Th contents might be a viable explanation.

Simple one-stage modeling of ancient silicate reservoirs forming significantly early in Earth's history always yields coupled ^{182}W - ^{142}Nd excess or deficits, due to higher incompatibility of both daughter

elements during crustal melting. This led Tusch et al. (2022) to propose a two-stage model, where mafic Hadean protocrust is later depleted by extraction of felsic protocrust, after the decay of $^{182}\mathrm{Hf}$ has ceased. Consequently, the short-lived Sm-Nd system may have been affected after the extinction of the Hf-W system. Such complex isotope systematics are also indicated by rocks from some Archean cratons that display deficits or modern mantle-like $\mu^{142}\mathrm{Nd}$ values although they have $^{182}\mathrm{W}$ excesses, showing that the systems are susceptible to decoupling (e.g., Leitzke et al., 2024; Reimink et al., 2018; Tusch et al., 2019, 2022). Thus, the observed decoupling of $^{142}\mathrm{Nd}$ - $^{182}\mathrm{W}$ deficits does not exclude the presence of recycled silicate components. As for short-lived isotope systems, long-lived isotope systems may also be susceptible to geological processes anytime from the Hadean to the present. This will be further evaluated with respect to $^{143}\mathrm{Nd}/^{144}\mathrm{Nd}$ systematics below.

Upon closer inspection, the Tusch et al. (2022) model can also account for the differences in $\epsilon^{143}Nd$ between the pristine DVP and La Réunion lavas. The mafic crustal restite in the original Tusch et al. (2022) model should evolve towards radiogenic $\varepsilon^{14\bar{3}}Nd$ compositions, which is not found in Group 3 DVP lavas (lower ε^{143} Nd). However, the modelled isotope composition of such restites is strongly affected by the degree of mantle melting that produced the mafic proto-crust and by the degree of melt depletion following the extraction of felsic melt producing the proto-crust restite. As indicated by the results of the model of Tusch et al. (2022), variations in the degree of mantle melting and felsic melt depletion produce modelled restite compositions extending from radiogenic to more unradiogenic ε^{143} Nd values and would also display lower W/Th and W/U ratios than the primitive mantle, matching the chemical compositions of DVP Group 3 (Fig 5). Such low W/Th and W/U would also be expected for a recycled mafic proto-crust, as W is expected to be transported away from the recycled material via fluids (König et al., 2008). Recycling of material that experienced Hadean silicate differentiation might have led to a variety of long-lived radiogenic isotope compositions, making these a less diagnostic test for the incorporation of proto-crustal restites on a global scale. In summary, such models need to be tested carefully for individual plume systems, but in our case can provide a viable explanation for the isotope compositions of DVP and La Réunion lavas (Fig 5b,c; Suppl. fig. 6, 7).

Summarizing the previous discussion, three models may explain the ¹⁸²W systematics in the Deccan-La Réunion plume (Fig. 6): 1) corederived W contributed to variable degrees to two chemically different lower mantle sources that were then tapped by the mantle plume at different timescales, 2) the La Réunion mantle source incorporated corederived W and an ancient restite reservoir was additionally added to the DVP Group 3 source (see also Peters et al., 2021) or 3) the Deccan-La Réunion source is dominated by a mafic restite reservoir best resembled by DVP Group 3 that was then altered by admixture of an additional mantle component or distinct lithospheric material producing La Réunion-like melt compositions. In all three scenarios, the isotope composition of DVP Group 2 is explained by the assimilation of crustal and lithospheric mantle components in the plume source or during the ascent through the Indian lithosphere. It is important to note that these three scenarios may provide an explanation for the isotope systematics of the Deccan-La Réunion plume but some of these scenarios may perhaps fail to explain the chemical compositions of other plume systems. Thus, there is a need to investigate plume systems individually from head to tail.

As mentioned by Willhite et al. (2024) for the Hawaiian plume where also co-variations of W with lithophile elements and isotope systems have been identified, neither a silicate component nor core-derived W for the source of the ¹⁸²W deficits can be fully excluded at this stage, which also applies to the Deccan-La Réunion plume. Nevertheless, due to the co-variation of W with Pb isotopes, and the trace element and isotope compositions of DVP Group 3 that are consistent with the incorporation of a proto-crustal restite component, we currently favor

the latter two models in explaining the 182 W deficits in the Deccan-La Réunion plume instead of a pure core-derived origin. However, with more data this view may change in the future.

6. Conclusion

New $\mu^{182}W$ and $\mu^{142}Nd$ data for flood basalts from the Deccan Volcanic Province (DVP) combined with new $\mu^{142}Nd$ and Pb isotope data for lavas from La Réunion that have been previously measured for $\mu^{182}W$ (Jansen et al., 2022) can shed new light on the geodynamic and chemical evolution of the Deccan-La Reunion plume from head to tail.

The Deccan-La Réunion plume displays variable deficits in $^{182}\mathrm{W}$, but no resolvable µ¹⁴²Nd anomalies were identified, in contrast to previous studies (e.g., Peters et al., 2018, 2021). For the DVP we identified two groups with resolvably distinct $\mu^{182}\mbox{W}$ compositions which are consistent with the previously suggested geochemical groups (Pakulla et al., 2023). DVP Group 2 lavas (μ^{182} W: -4.2 ± 3.0 , 95 % CI) are unresolvable from compositions of La Réunion basalts ($\mu^{182}W$: -4.9 ± 1.5 , 95 % CI). DVP Group 3 samples exhibit resolvably lower $\mu^{182}W$ values of -10.1 ± 2.6 (95 % CI) and mark the plume-derived endmember. Mixing calculations suggest that Group 2 samples can be explained by the admixture of lithospheric mantle material and crust to a Group 3-like composition. Contrarily, the DVP Group 3 endmember has low u¹⁸²W, low $^{206}\text{Pb}/^{204}\text{Pb}$ ratios, and lower $\Delta^{207}\text{Pb}/^{206}\text{Pb}$ than the typical Indian upper mantle and La Réunion melts, and we propose that these isotope systematics can be explained by core-mantle interaction affecting distinct reservoirs, by the involvement of a recycled Hadean mafic component, or by a combination of a recycled Hadean component and core-mantle interaction (Fig. 6). Due to coupled variations in Pb isotopes and ¹⁸²W as well as somewhat lower W/Th ratios in DVP Group 3 samples, we currently favor models that involve the presence of a recycled Hadean mafic component. Thus, future studies on combined short- and long-lived isotope systematics as well as He isotopes investigating the long-term evolution of mantle plumes will be the key to unravelling the origin of the anomalous $\mu^{182}W$ and $\mu^{142}Nd$ compositions found in deep-rooted mantle plumes.

CRediT authorship contribution statement

Josua J. Pakulla: Writing – review & editing, Writing – original draft, Visualization, Validation, Investigation, Formal analysis, Data curation, Conceptualization. Jonas Tusch: Writing – review & editing, Methodology, Investigation. Eric Hasenstab-Dübeler: Writing – review & editing, Methodology, Investigation. Arathy Ravindran: Writing – review & editing, Investigation, Resources. Mike W. Jansen: Writing – review & editing, Resources, Conceptualization. Felipe P. Leitzke: Writing – review & editing, Resources. Raymond A. Duraiswami: Writing – review & editing, Resources. Carsten Münker: Writing – review & editing, Supervision, Resources, Project administration, Funding acquisition, Conceptualization, Formal analysis.

Declaration of competing interest

The authors declare that they have no known competing financial interests or personal relationships that could have appeared to influence the work reported in this paper.

Acknowledgements

J.J.Pakulla and C.Münker acknowledge funding from the Deutsche Forschungsgemeinschaft, projects MU1406/22–1 and MU1406/23–1 (SPP 2404 "DeepDyn"). We are also grateful to Frank Wombacher and Mario Fischer-Gödde for help with the instruments and Ruiyu Yang, Max

Hellers, and Almut Katzemich for their help in the lab. J.J.Pakulla is also thankful for fruitful discussions with Elis Hoffman and Barbara Romanowicz which provided a new perspective on this manuscript. We appreciate the constructive and helpful comments by four anonymous reviewers that improved the manuscript and the editorial handling by Frédéric Moynier and Fang-Zhen Teng.

Supplementary materials

Supplementary material associated with this article can be found, in the online version, at doi:10.1016/j.epsl.2025.119225.

Data availability

Data will be made available on request.

References

- Andreasen, R., Sharma, M., Subbarao, K.V., Viladkar, S.G., 2008. Where on Earth is the enriched Hadean reservoir? Earth. Planet. Sci. Lett. 266 (1-2), 14–28.
- Ballmer, M.D., Houser, C., Hernlund, J.W., Wentzcovitch, R.M., Hirose, K., 2017. Persistence of strong silica-enriched domains in the Earth's lower mantle. Nat. Geosci. 10 (3), 236–240.
- Basu, A.R., Renne, P.R., Dasgupta, D.K., Teichmann, F., Poreda, R.J., 1993. Early and Late Alkali Igneous Pulses and a High-3He Plume Origin for the Deccan Flood Basalts. Science (1979) 261 (5123), 902–906.
- Basu, A.R., Saha-Yannopoulos, A., Chakrabarty, P., 2020. A precise geochemical volcanostratigraphy of the Deccan traps. Lithos. 376–377.
- Bennett, V.C., Brandon, A.D., Nutman, A.P., 2007. Coupled 142Nd-143Nd isotopic evidence for Hadean mantle dynamics. Science (1979) 318 (5858), 1907–1910.
- Bosch, D., Blichert-Toft, J., Moynier, F., Nelson, B.K., Telouk, P., Gillot, P.Y., Albarède, F., 2008. Pb, Hf and Nd isotope compositions of the two Réunion volcanoes (Indian Ocean): A tale of two small-scale mantle "blobs"? Earth. Planet. Sci. Lett. 265 (3-4), 748–765.
- Brandon, A.D., Walker, R.J., 2005. The debate over core–mantle interaction. Earth. Planet. Sci. Lett. 232 (3-4), 211–225.
- Brandon, A.D., Walker, R.J., Morgan, J.W., Norman, M.D., Prichard, H.M., 1998. Coupled 186Os and 187Os evidence for core-mantle interaction. Science (1979) 280 (5369), 1570–1573.
- Brandon, A.D., Walker, R.J., Puchtel, I.S., Becker, H., Humayun, M., Revillon, S., 2003. 1860s–1870s systematics of Gorgona Island komatiites: implications for early growth of the inner core. Earth. Planet. Sci. Lett. 206 (3-4), 411–426.
- Bredow, E., Steinberger, B., Gassmöller, R., Dannberg, J., 2017. How plume-ridge interaction shapes the crustal thickness pattern of the Réunion hotspot track. Geochemistry, Geophysics, Geosystems 18 (8), 2930–2948.
- Caro, G., Bourdon, B., Birck, J.L., Moorbath, S., 2006. High-precision 142Nd/144Nd measurements in terrestrial rocks: Constraints on the early differentiation of the Earth's mantle. Geochim. Cosmochim. Acta 70 (1), 164–191.
- Chiera, N.M., Sprung, P., Amelin, Y., Dressler, R., Schumann, D., Talip, Z., 2024. The 146Sm half-life re-measured: consolidating the chronometer for events in the early Solar System. Sci. Rep. 14 (1), 17436.
- Cipriani, A., Bonatti, E., Carlson, R.W., 2011. Nonchondritic 142 Nd in suboceanic mantle peridotites. Geochemistry, Geophysics, Geosystems 12 (3) n/a-n/a.
- Cox, K.G., Hawkesworth, C.J., 1985. Geochemical Stratigraphy of the Deccan Traps at Mahabaleshwar, Western Ghats, India, with Implications for Open System Magmatic Processes. Journal of Petrology 26 (2), 355–377.
- Deng, J., Du, Z., 2023. Primordial helium extracted from the Earth's core through magnesium oxide exsolution. Nat. Geosci. 16 (6), 541–545.
- Dupré, B., Allègre, C.J., 1983. Pb–Sr isotope variation in Indian Ocean basalts and mixing phenomena. Nature 303 (5913), 142–146.
- Friedman, A.M., Milsted, J., Metta, D., Henderson, D., Lerner, J., Harkness, A.L., Rok Op, D.J., 1966. Alpha Decay Half Lives of 148 Gd 150 Gd and 146 Sm. Radiochim. Acta 5 (4), 192–194.
- Garçon, M., Boyet, M., Carlson, R.W., Horan, M.F., Auclair, D., Mock, T.D., 2018. Factors influencing the precision and accuracy of Nd isotope measurements by thermal ionization mass spectrometry. Chemical Geology 476, 493–514.
- Hart, S.R., 1984. A large-scale isotope anomaly in the Southern Hemisphere mantle. Nature 309 (5971), 753–757.
- Hasenstab-Dübeler, E., Tusch, J., Hoffmann, J.E., Fischer-Gödde, M., Szilas, K., Münker, C., 2022. Temporal evolution of 142Nd signatures in SW Greenland from high precision MC-ICP-MS measurements. Chemical Geology 614, 121141.
- Herret, M.T., Peters, B.J., Kim, D., Castillo, P.R., Mundl-Petermeier, A., 2023. Decoupling of short-lived radiogenic and helium isotopes in the Marquesas hotspot. Chemical Geology 640, 121727.
- Hofmann, A.W., Class, C., Goldstein, S.L., 2022. Size and composition of the MORB+OIB mantle reservoir. Geochemistry, Geophysics, Geosystems.
- Hofmann, A.W., Jochum, K.P., Seufert, M., White, W.M., 1986. Nb and Pb in oceanic basalts: new constraints on mantle evolution. Earth. Planet. Sci. Lett. 79 (1-2), 33–45.

- Horan, M.F., Carlson, R.W., Walker, R.J., Jackson, M., Garçon, M., Norman, M., 2018. Tracking Hadean processes in modern basalts with 142-Neodymium. Earth. Planet. Sci. Lett. 484, 184–191.
- Hoyer, P.A., Haase, K.M., Regelous, M., Fluteau, F., 2023. Systematic and Temporal Geochemical Changes in the Upper Deccan Lavas: Implications for the Magma Plumbing System of Flood Basalt Provinces. Geochemistry, Geophysics, Geosystems 24 (2)
- Humayun, M., 2011. A model for osmium isotopic evolution of metallic solids at the core-mantle boundary. Geochemistry, Geophysics, Geosystems 12 (3).
- Ireland, T.J., Walker, R.J., Brandon, A.D., 2011. 1860s-1870s systematics of Hawaiian picrites revisited: New insights into Os isotopic variations in ocean island basalts. Geochim. Cosmochim. Acta 75 (16), 4456-4475.
- Jackson, M.G., Blichert-Toft, J., Halldorsson, S.A., Mundl-Petermeier, A., Bizimis, M., Kurz, M.D., Price, A.A., Harethardottir, S., Willhite, L.N., Breddam, K., Becker, T.W., Fischer, R.A., 2020. Ancient helium and tungsten isotopic signatures preserved in mantle domains least modified by crustal recycling. Proc. Natl. Acad. Sci. u S. a 117 (49), 30993–31001.
- Jansen, M.W., Münker, C., Pakulla, J.J., Hasenstab-Dübeler, E., Marien, C.S., Schulz, T., Kirchenbaur, M., Schneider, K.P., Tordy, R., Schmitt, V., Wombacher, F., 2024. Petrogenesis of volcanic rocks from the Quaternary Eifel volcanic fields, Germany: detailed insights from combined trace-element and Sr-Nd-Hf-Pb-Os isotope data. Contributions to Mineralogy and Petrology 179 (6), 57.
- Jansen, M.W., Tusch, J., Münker, C., Bragagni, A., Avanzinelli, R., Mastroianni, F., Stuart, F.M., Kurzweil, F., 2022. Upper mantle control on the W isotope record of shallow level plume and intraplate volcanic settings. Earth. Planet. Sci. Lett. 585.
- Jenner, F.E., O'Neill, H.S.C., 2012. Analysis of 60 elements in 616 ocean floor basaltic glasses. Geochemistry, Geophysics, Geosystems 13 (2) n/a-n/a.
- Jones, T.D., Davies, D.R., Sossi, P.A., 2019. Tungsten isotopes in mantle plumes: Heads it's positive, tails it's negative. Earth. Planet. Sci. Lett. 506, 255–267.
- König, S., Münker, C., Schuth, S., Garbe-Schönberg, D., 2008. Mobility of tungsten in subduction zones. Earth. Planet. Sci. Lett. 274 (1-2), 82–92.
- Labrosse, S., Hernlund, J.W., Coltice, N., 2007. A crystallizing dense magma ocean at the base of the Earth's mantle. Nature 450 (7171), 866–869.
- Lassiter, J., 2006. Constraints on the coupled thermal evolution of the Earth's core and mantle, the age of the inner core, and the origin of the 1860s/1880s "core signal" in plume-derived lavas. Earth. Planet. Sci. Lett. 250 (1-2), 306–317.
- Leitzke, F.P., Pakulla, J.J., Tusch, J., Ravindran, A., Gordilho-Barbosa, R., Zincone, S.A., Hellers, M., Martins, A.A., Spreafico, R.R., Yang, R., Wombacher, F., Barbosa, J., Münker, C., 2024. Evidence for a missing late veneer from 182W and 142Nd systematics in the Archean S\u00e4o Francisco Craton. Earth. Planet. Sci. Lett. 647, 119022.
- Li, Y., Vočadlo, L., Ballentine, C., Brodholt, J.P., 2022. Primitive noble gases sampled from ocean island basalts cannot be from the Earth's core. Nat. Commun. 13 (1), 3770.
- Lugmair, G.W., Carlson, R.W., 1978. The Sm-Nd history of KREEP. Lunar and Planetary Science Conference 689–704.
- Luguet, A., Graham Pearson, D., Nowell, G.M., Dreher, S.T., Coggon, J.A., Spetsius, Z.V., Parman, S.W., 2008. Enriched Pt-Re-Os isotope systematics in plume lavas explained by metasomatic sulfides. Science (1979) 319 (5862), 453–456.
- Meen, J.K., Rogers, J.J., Fullagar, P.D., 1992. Lead isotopic compositions of the Western Dharwar craton, southern India: Evidence for distinct Middle Archean terranes in a Late Archean craton. Geochim. Cosmochim. Acta 56 (6), 2455–2470.
- Melluso, L., Mahoney, J.J., Dallai, L., 2006. Mantle sources and crustal input as recorded in high-Mg Deccan Traps basalts of Gujarat (India). Lithos. 89 (3-4), 259–274.
- Mittal, T., Richards, M.A., Fendley, I.M., 2021. The Magmatic Architecture of Continental Flood Basalts I: Observations From the Deccan Traps. JGR Solid Earth 126 (12).
- Mundl, A., Touboul, M., Jackson, M.G., Day, J.M.D., Kurz, M.D., Lekic, V., Helz, R.T., Walker, R.J., 2017. Tungsten-182 heterogeneity in modern ocean island basalts. Science (1979) 356 (6333), 66–69.
- Mundl, A., Walker, R.J., Reimink, J.R., Rudnick, R.L., Gaschnig, R.M., 2018. Tungsten-182 in the upper continental crust: Evidence from glacial diamictites. Chemical Geology 494, 144–152.
- Mundl-Petermeier, A., Halldorsson, S.A., Castillo, P.R., Walker, R.J., Ackerman, L., Koeberl, C., 2020a. Decoupled He-W isotope systematics in the East African Rift System. AGU Fall Meeting Abstracts.
- Mundl-Petermeier, A., Walker, R.J., Fischer, R.A., Lekic, V., Jackson, M.G., Kurz, M.D., 2020b. Anomalous 182W in high 3He/4He ocean island basalts: Fingerprints of Earth's core? Geochim. Cosmochim. Acta 271, 194–211.
- Mundl-Petermeier, A., Walker, R.J., Jackson, M.G., Blichert-Toft, J., Kurz, M.D., Halldórsson, S.A., 2019. Temporal evolution of primordial tungsten-182 and 3He/4He signatures in the Iceland mantle plume. Chemical Geology 525, 245–259.
- Otsuka, K., Karato, S., 2012. Deep penetration of molten iron into the mantle caused by a morphological instability. Nature 492 (7428), 243–246.
- Pakulla, J.J., Jansen, M.W., Duraiswami, R.A., Gadpallu, P., Tusch, J., Jentzsch, C., Braukmüller, N., Wombacher, F., Münker, C., 2023. Trace element and Sr-Nd-Hf-Pb isotope evidence for a multi-magma chamber system beneath the Deccan Volcanic Province. India. Chemical Geology 640, 121749.
- Paul, J., Ghosh, A., 2021. Could the Réunion plume have thinned the Indian craton? Geology. 50 (3), 346–350.
- Peng, Z.X., Mahoney, J., Hooper, P., Harris, C., Beane, J., 1994. A role for lower continental crust in flood basalt genesis? Isotopic and incompatible element study of the lower six formations of the western Deccan Traps. Geochim. Cosmochim. Acta 58 (1), 267–288.
- Peng, Z.X., Mahoney, J.J., Hooper, P.R., Macdougall, J.D., Krishnamurthy, P., 1998.
 Basalts of the northeastern Deccan Traps, India: Isotopic and elemental geochemistry

- and relation to southwestern Deccan stratigraphy. Journal of Geophysical Research: Solid Earth 103 (B12), 29843–29865.
- Peng, Y., Yoshino, T., Deng, J., 2024. Grain boundary diffusion cannot explain the W isotope heterogeneities of the deep mantle. Research Square. https://doi.org/10.21203/rs.3.rs-4517988/v1.
- Peters, B.J., Carlson, R.W., Day, J.M.D., Horan, M.F., 2018. Hadean silicate differentiation preserved by anomalous 142Nd/144Nd ratios in the Réunion hotspot source. Nature 555 (7694), 89–93.
- Peters, B.J., Day, J.M.D., 2017. A geochemical link between plume head and tail volcanism. Geochem. Perspect. Lett. 29–34.
- Peters, B.J., Day, J.M.D., Greenwood, R.C., Hilton, D.R., Gibson, J., Franchi, I.A., 2017. Helium-oxygen-osmium isotopic and elemental constraints on the mantle sources of the Deccan Traps. Earth. Planet. Sci. Lett. 478, 245–257.
- Peters, B.J., Mundl-Petermeier, A., Carlson, R.W., Walker, R.J., Day, J.M.D., 2021. Combined Lithophile-Siderophile Isotopic Constraints on Hadean Processes Preserved in Ocean Island Basalt Sources. Geochemistry, Geophysics, Geosystems 22 (3).
- Peters, D., Rizo, H., O'Neil, J., Hamelin, C., Shirey, S.B., 2024. Comparative 142Nd and 182W study of MORBs and the 4.5 Gyr evolution of the upper mantle. Geochem. Persp. Let. 29, 51–56.
- Pfänder, J.A., Münker, C., Stracke, A., Mezger, K., 2007. Nb/Ta and Zr/Hf in ocean island basalts — Implications for crust–mantle differentiation and the fate of Niobium. Earth. Planet. Sci. Lett. 254 (1-2), 158–172.
- Ravindran, A., Mezger, K., Balakrishnan, S., Berndt, J., Ranjan, S., Upadhyay, D., 2023. Formation of Paleo- to Meso-Archean continental crust in the western Dharwar Craton, India: Constraints from U Pb zircon ages and Hf-Pb-Sr isotopes of granitoids and sedimentary rocks. Chemical Geology 615, 121196.
- Reimink, J.R., Chacko, T., Carlson, R.W., Shirey, S.B., Liu, J., Stern, R.A., Bauer, A.M., Pearson, D.G., Heaman, L.M., 2018. Petrogenesis and tectonics of the Acasta Gneiss Complex derived from integrated petrology and 142Nd and 182W extinct nuclidegeochemistry. Earth. Planet. Sci. Lett. 494, 12–22.
- Rizo, H., Andrault, D., Bennett, N.R., Humayun, M., Brandon, A., Vlastelic, I., Moine, B., Poirier, A., Bouhifd, M.A., Murphy, D.T., 2019. 182W evidence for core-mantle interaction in the source of mantle plumes. Geochem. Persp. Let. 6–11.
- Saji, N.S., Wielandt, D., Paton, C., Bizzarro, M., 2016. Ultra-high-precision Nd-isotope measurements of geological materials by MC-ICPMS. J. Anal. At. Spectrom. 31 (7), 1490–1504.
- Schoene, B., Eddy, M.P., Samperton, K.M., Keller, C.B., Keller, G., Adatte, T., Khadri, S.F. R., 2019. U-Pb constraints on pulsed eruption of the Deccan Traps across the end-Cretaceous mass extinction. Science (1979) 363 (6429), 862–866.
- Schuth, S., König, S., Münker, C., 2011. Subduction zone dynamics in the SW Pacific plate boundary region constrained from high-precision Pb isotope data. Earth. Planet. Sci. Lett. 311 (3-4), 328–338.
- Sharma, J., Kumar, M.R., Roy, K.S., Roy, P.N.S., 2018. Seismic Imprints of Plume-Lithosphere Interaction Beneath the Northwestern Deccan Volcanic Province. Journal of Geophysical Research: Solid Earth 123 (12), 10,831-10,853.
- Sheth, H.C., Pande, K., 2014. Geological and 40Ar/39Ar age constraints on late-stage Deccan rhyolitic volcanism, inter-volcanic sedimentation, and the Panvel flexure from the Dongri area, Mumbai. J. Asian Earth. Sci. 84, 167–175.

- Srivastava, R.K., Wang, F., Shi, W., 2020. Substantiation of Réunion plume induced prolonged magmatic pulses (ca. 70.5–65.5 Ma) of the Deccan LIP in the Chhotanagpur Gneissic Complex, eastern India: Constraints from 40Ar/39Ar geochronology. Journal of Earth System Science 129 (1).
- Su, Y., Ni, S., Zhang, B., Chen, Y., Wu, W., Li, M., Sun, H., Hou, M., Cui, X., Sun, D., 2024. Detections of ultralow velocity zones in high-velocity lowermost mantle linked to subducted slabs. Nat. Geosci. 17 (4), 332–339.
- Tanaka, T., Togashi, S., Kamioka, H., Amakawa, H., Kagami, H., Hamamoto, T., Yuhara, M., Orihashi, Y., Yoneda, S., Shimizu, H., Kunimaru, T., Takahashi, K., Yanagi, T., Nakano, T., Fujimaki, H., Shinjo, R., Asahara, Y., Tanimizu, M., Dragusanu, C., 2000. JNdi-1: a neodymium isotopic reference in consistency with LaJolla neodymium. Chemical Geology 168 (3-4), 279–281.
- Tusch, J., Hoffmann, J.E., Hasenstab, E., Fischer-Gödde, M., Marien, C.S., Wilson, A.H., Münker, C., 2022. Long-term preservation of Hadean protocrust in Earth's mantle. Proc. Natl. Acad. Sci. u S. a 119 (18), e2120241119.
- Tusch, J., Munker, C., Hasenstab, E., Jansen, M., Marien, C.S., Kurzweil, F., van Kranendonk, M.J., Smithies, H., Maier, W., Garbe-Schonberg, D., 2021. Convective isolation of Hadean mantle reservoirs through Archean time. Proc. Natl. Acad. Sci. u S a 118 (2)
- Tusch, J., Sprung, P., van de Löcht, J., Hoffmann, J.E., Boyd, A.J., Rosing, M.T., Münker, C., 2019. Uniform 182W isotope compositions in Eoarchean rocks from the Isua region, SW Greenland: The role of early silicate differentiation and missing late veneer. Geochim. Cosmochim. Acta 257, 284–310.
- Vockenhuber, C., Oberli, F., Bichler, M., Ahmad, I., Quitté, G., Meier, M., Halliday, A.N., Lee, D.C., Kutschera, W., Steier, P., Gehrke, R.J., Helmer, R.G., 2004. New half-life measurement of 182Hf: improved chronometer for the early solar system. Phys. Rev. Lett. 93 (17), 172501.
- Walker, R.J., Mundl-Petermeier, A., Puchtel, I.S., Nicklas, R.W., Hellmann, J.L., Echeverría, L.M., Ludwig, K.D., Bermingham, K.R., Gazel, E., Devitre, C.L., Jackson, M.G., Chauvel, C., 2023. 182W and 1870s constraints on the origin of siderophile isotopic heterogeneity in the mantle. Geochim. Cosmochim. Acta 363, 15–39.
- Wang, D., Carlson, R.W., 2022. Tandem-column extraction chromatography for Nd separation: minimizing mass-independent isotope fractionation for ultrahighprecision Nd isotope-ratio analysis. J. Anal. At. Spectrom. 37 (1), 185–193.
- White, R., McKenzie, D., 1989. Magmatism at rift zones: The generation of volcanic continental margins and flood basalts. J. Geophys. Res. 94 (B6), 7685–7729.
- Willbold, M., Elliott, T., Moorbath, S., 2011. The tungsten isotopic composition of the Earth's mantle before the terminal bombardment. Nature 477 (7363), 195–198.
- Willhite, L.N., Finlayson, V.A., Walker, R.J., 2024. Evolution of tungsten isotope systematics in the Mauna Kea volcano provides new constraints on anomalous μ182W and high 3He/4He in the mantle. Earth. Planet. Sci. Lett. 640, 118795.
- Williams, C.D., Li, M., McNamara, A.K., Garnero, E.J., van Soest, M.C., 2015. Episodic entrainment of deep primordial mantle material into ocean island basalts. Nat. Commun. 6, 8937.
- Wolf, J., Long, M.D., Frost, D.A., 2024. Ultralow velocity zone and deep mantle flow beneath the Himalayas linked to subducted slab. Nat. Geosci. 17 (4), 302–308.
- Yoshino, T., Makino, Y., Suzuki, T., Hirata, T., 2020. Grain boundary diffusion of W in lower mantle phase with implications for isotopic heterogeneity in oceanic island basalts by core-mantle interactions. Earth. Planet. Sci. Lett. 530, 115887.